RESEARCH AND APPLICATION OF THE EVAPORATION CAPACITY SPATIAL INTERPOLATION METHOD FOR AGRICULUTRAL ENVIRONMENT
/
面向农业环境的蒸发量空间插值方法研究和应用

Ph.D. Yinlong JIN[1)], Prof. Ph.D. Eng. Jiesheng HUANG[1)], Ph.D. Ben LI[1,2)]
[1)]State Key Laboratory of Water Resource and Hydropower Engineering Science ,Wuhan University, Wuhan / China;
[2)] College of Earth, Ocean, and Atmospheric Sciences, Oregon State University, Corvallis / U.S.A.
Tel: +86-138-71136226; E-mail:wrhjinyl@whu.edu.cn

Keywords: *Agricultural environment; Waterlogging field; Evaporation capacity; Spatial interpolation*

ABSTRACT

Waterlogging is a common agricultural disaster with complicated causes when agricultural environment changes, one of which is evaporation. Identifying waterlogging disasters requires evaporation data with continuous space–time distribution. Traditional spatial interpolation methods are based on the correlation between the interpolating point and observation station. By contrast, the present study develops a new method by conducting the following work: First, ground evaporation and air temperature are considered to be a field coupled with the atmospheric flow field, which is calculated through the spectral method. A new spatial interpolation method is proposed based on spherical harmonics and with the incorporation of temperature parameters into the calculation model. Second, the internal and external errors of the interpolation results are calculated under multiple temperature conditions, and precision evaluation and robustness analysis are conducted on the interpolation results of the daily evaporation capacity. Lastly, a comparative analysis is conducted on the calculation results of the monthly evaporation capacity and MOD16 data under multiple temperature conditions. This study provides selection methods and judging conditions for temperature parameters and also discusses the occurrence of the temperature accumulative effect in the interpolation of the monthly evaporation capacity. This study also explains the contracting phenomenon of the residual distribution and model precision, as well as the temperature accumulation phenomenon, in the interpolation of the monthly evaporation capacity. The experimental results show that the method proposed in this study is a feasible and effective spatial interpolation method for evaporation capacity and can provide scientific basis for the farming and water management.

摘要

农田环境变化时，涝渍灾害是常见的成因复杂的农业灾害，蒸发是重要的致灾因素．渍害的识别需要时空连续分布的蒸发量数据,传统的空间插值方法依据插值点与观测站之间的相关性，本文寻求新思路并进行了以下工作：首先，从大气运动场解算的谱方法，将地面蒸发和大气温度看做一个耦合场，提出一种基于球谐函数的空间插值新方法，同时将温度参数纳入解算模型．再者，计算多种温度条件下插值结果的内外符合精度，对日蒸发量插值结果进行精度评价和稳健性分析．最后，对多种温度条件下的月蒸发量计算结果和MOD16数据进行对比分析，给出了温度参数选择方法判定条件，同时提出了月蒸发量插值计算中的温度累积效应．同时解释了残差分布与模型精度的相悖现象和月蒸发量插值中的温度累积现象．实验结果表明本文研究方法是一种可行且有效蒸发量空间插值算法，可为农业水管理提供科学依据。

INTRODUCTION

Many studies focus on agriculture environment, where the long-term saturation state of soil moisture in the crop root system restricts crop growth and reduces crop productivity *(Qian and Wang, 2015).* Field evaporation is a key link in the water circulation process and a significant component of water circulation. Along with rainfall and runoff, it determines the hydrologic balance in a region and directly influences farmland environment. Under certain topographic and rainfall conditions, a continuously low evaporation capacity results in long-term soil water saturation. This then leads to waterlogging disasters and causes crop failure, while a continuously high evaporation would result in droughts as well as crop failure. Hence, changing the process and features of evaporation capacity is the main basis for field water applications and management, and research on evaporation capacity is of great importance to agricultural production *(Su and Feng, 2015)*.

At present, many methods to calculate evaporation capacity are available. The most direct method is the instrument measurement method, which involves the use of an evaporation pan and land evaporator to

directly measure the evaporation capacity. In the case of insufficient or lack of measured data, the indirect method can also be used to estimate the evaporation capacity. The methods with the broadest application are the Penman–Monteith (P-M) formula, which is the only standard for calculating ET0 suggested by Food and Agriculture Organization of the United Nations (FAO), and the Hargreaves (H-S) formula, which can calculate the daily ET0; the former requires seven meteorological factors, and the latter needs four meteorological factors. Moreover, remote sensing technology, together with meteorological data, under a certain assumption, may employ the water-vapour balance equation, geostatistics theory, or all kinds of regression methods to conduct spatial interpolation and thereby estimate the evaporation capacity within a large scale *(Hassan, 2012)*. The aforementioned methods have their own advantages and limitations. When empirical methods, such as the P-M formula, are used, the physical conditions of various regions must necessarily be considered. Hence, such methods are quite difficult to apply when the evaporation capacity has a large variation. When remote sensing inversion or the water-vapour balance equation is used to estimate the evaporation capacity, the model needs multiple parameters with a complicated model structure. The development of remote sensing and GIS technology can realize the acquisition of large-scale evaporation capacity data; however, such acquisition remains very difficult to realize given continuously changing large-scale evaporation capacity data and the restrictions imposed by ground data and meteorological conditions *(Raghuveer et al., 2011; Paul et al., 2012).*

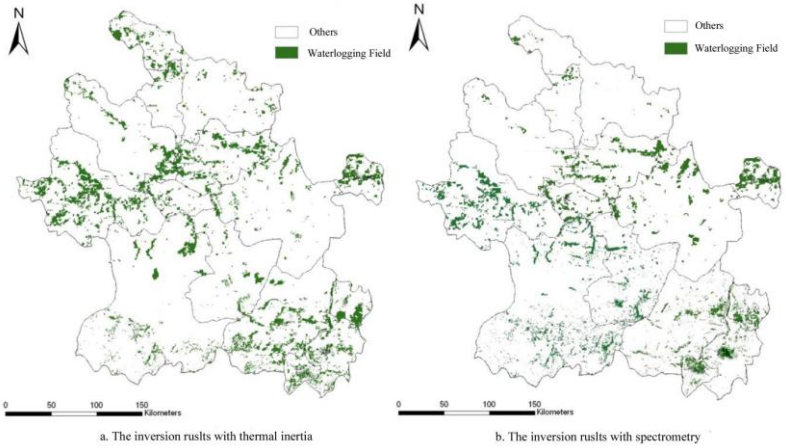

Fig.1 - Distribution diagram of the inversion results for the waterlogging field

Waterlogging control, drought resistance, and disaster reduction have always been important in the field of agricultural production research. Fig.1 shows the inversion results of using evaporation data with continuous space–time distribution and other multi-source data on waterlogging fields in Anhui Province *(Jin et al, 2014)*. Many spatial interpolation methods exist, such as the Thiessen polygon, spline function method, inverse distance weighted (IWD), Kriging, spatial interpolation model of artificial neural network (BPNNSI), and so on. The relevant assumptions of the aforementioned methods are based on the spatial distribution and location of evaporation capacity, which is then solved by the methods by considering the other factors that influence it *(Cha, 2011).* The results obtained are limited to some data of observation stations near the interpolation point with obvious uncertainty. The present study proposes a spatial interpolation method based on the spherical function, which considers evaporation capacity as a field covering the whole interpolation area, and the using spectral method to solve the overall parameters. It also integrates temperature data to further reduce the uncertainty of the calculation results *(Tian, 2012).* Anhui is located in a transitional area of warm temperature zone with an average annual temperature of 14–16 °C and a temperature difference of 2 °C between the south and north.

MATERIAL AND METHOD

Data source

The temperature dataset “China daily surface air temperature value 0.5°×0.5°grid point dataset (V2.0)” was downloaded from the Chinese meteorological data shared service network, and the basic meteorological element data from 2,472 open sea stations (i.e., excluding Xisha and Coral Island) and from the latest national-level surface meteorological stations reorganized on the basis of special database.

The evaporation capacity data were derived from two sources. The first source was the daily

evaporation capacity data from 26 meteorological stations in Anhui Province downloaded from the Anhui drought severity information network. The second dataset, the MOD16 data (transpiration product) provided by MODIS with a spatial resolution of 1 km for a period of months, could be directly downloaded from the website provided by MODIS. The MOD16 data from May to August of 2013 were selected for the experiment in this study.

Data preprocessing

The downloaded temperature data consisted of ASCII coded documents, which could directly be read. The transformation of the format and spatial data had to be conducted, and the internal grid data files (*.img) supported by the ARCGIS platform were generated. The MOD16 data were also subjected to file format transformation, reprojection, and splicing, and clipping work, depending on the ARCGIS platform. The spatial datum was introduced for the convenience of analysis in this study. The spatial datum involved in this paper consisted of GCS_WGS_1984.

Spatial interpolation method based on spherical harmonic function

The research on evaporation began with bare land evaporation, using the empirical and mechanism method. The development of this line of research showed, that the evapotranspiration problem of crops was closely related to bare land evaporation. Researchers introduced the energy balance method and water vapour diffusion theory to the research on evapotranspiration. The evapotranspiration quantity of crops is considered to indicate the process of energy consumption; the water yield consumed by crop evapotranspiration is calculated through energy balance (*Li et al., 2013; Yang, 2011*).

Based on the aforementioned analysis, various corresponding transpiration formulas are available for different phases of crop evapotranspiration. Under normal conditions, the calculation of evaporation on bare soil uses the formula similar to that of crops:

$$E = k(e_1 - e_2) \tag{1}$$

where *E* is the crop evapotranspiration quantity, [mm]; *k* is a constant, [mm/hPa]; e_1 is the saturation vapour pressure and e_2 is the actual vapour pressure, [hPa].

Based on the Magnus formula (2), e_1 is a function of temperature:

$$e_1 = 6.1 \times 10^{\frac{7.45t}{t+273.16}} \tag{2}$$

where *t* is the daily average temperature in ^{o}C. Within the variation range of the meteorological temperature, the Magnus formula can be replaced by a straight line, and Equation (2) is transformed into

$$e_1 = Ct + D \tag{3}$$

where *C* is a constant, [hPa/K] and *D* is a constant, [hPa].

In Equation (1), the variation of the absolute value of e_2 is smaller than that of e_1, and its absolute value can be expressed with a constant. The above equation is substituted into (1), and the following can be obtained:

$$E = mt + n \tag{4}$$

where *m* is a constant, [mm/K] and *n* is a constant, [mm].

As shown above, the direct factors that influence the calculation of transpiration involve air pressure and temperature, so that atmospheric factors, such as temperature, should be considered in the spatial expansion of the transpiration data. The models used to predict evapotranspiration are divided into two types: The first involves direct calculation, such as the air humidity method, temperature wind speed method, and others; the second involves the determination of the total evapotranspiration quantity and crop factors of the reference crop, such as the P-M formula, complementary correlation theory, SPAC theory, evapotranspiration method for the reference crop, remote sensing method, and so on *(Lagos et al., 2013; Seitz, 2008)*. This study considers evaporation to consist of a field covering the surface of the earth and uses the spherical function model to solve the parameters of this field to realize the expansion of the evaporation data from a single observation station to continuous coverage.

The spherical function has been widely applied to the resolution of field equations, such as earth physics and atmospheric motion, among others. Compared with the classical grid method, the spectral method of the spherical function features high precision, good stability, and simple resolution *(Tolk, 2015; Seitz, 2008)*. The spherical function is adopted in this study to establish the basic model. By considering the relationship between evaporation and temperature, spatial distribution models (with or without consideration of temperature) are established, and the resolution results are then analyzed.

When the influence of temperature is not considered, the evaporation calculation model can be called a purely spherical function model and is expanded into the following form:

$$ET(\beta,s)=\sum_{n=0}^{n_{\max}}\sum_{m=0}^{n}\tilde{P}_{nm}(\sin\beta)(a_{nm}\cos(ms)+b_{nm}\sin(ms)) \quad (5)$$

where $ET(\beta,s)$ is the evapotranspiration in the observation station, [mm]; $n_{\max}$ is the order of the spherical harmonic function; $\tilde{P}_{nm}=\Lambda(n,m)P_{nm}$ is the normalized Legendre polynomial; Λ is the normalized function; P_{nm} is the normalized Legendre function; (β,s) is the geographic latitude and longitude of the observation station; and a_{nm} and b_{nm} are the coefficients to be resolved.

$$\Lambda(n,m)=\sqrt{2\frac{2n+1}{1+\delta_{nm}}\cdot\frac{(n-m)!}{(n+m)!}} \quad (6)$$

In the equation, δ_{nm} is the Kronecker function.

Considering the influence of temperature factors on evapotranspiration and the relationship expressed in Equation (4), the influence of temperature is integrated into Equation (5), and it can be called the expandable spherical function model, as shown in the following equation:

$$ET(\beta,s)=\sum_{n=0}^{n_{\max}}\sum_{m=0}^{n}\tilde{P}_{nm}(\sin\beta)(a_{nm}\cos(ms)+b_{nm}\sin(ms))+\mu T \quad (7)$$

where T is the temperature of the observation station, [K]; and μ is the coefficient to be resolved, [mm/K]. The other symbols are also found in Equation (5).

Model resolution

The specific flow of the model resolution flow is shown in Fig.2.

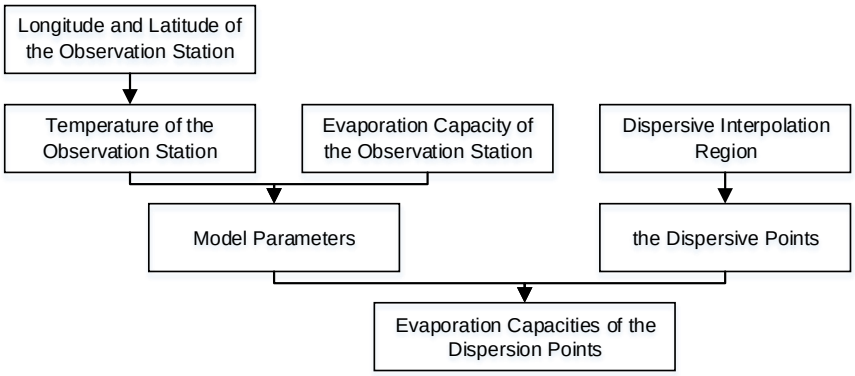

Fig.2 - Flow chart of the model resolution

The specific steps of the model resolution are as follows: First, the spatial analysis function of ARCGIS software is used to extract the temperature data. Second, the parameters in Equation (5) and (7) are re-resolved with the combination of the longitude and latitude and the measured value of evaporation. One group of parameters corresponds to one day. A total of nine coefficients are used when the temperature is not considered, and ten when the temperature is considered. The administrative region in An'hui Province is then dispersed, and the longitudinal and latitudinal coordinates and temperature values at the dispersed point are obtained. The evaporation capacity at this point is determined according to the parameters.

RESULTS

Model precision analysis

To evaluate the effectiveness of this model, the data from 23 observation stations, which are evenly distributed among the 26 observation stations in Anhui Province, are adopted to conduct mathematical modelling and calculation. The other three are used to conduct externally coincident inspections and to measure the precision of the model. Considering five day's worth of data from August 25 to 29, 2013, the compensating computation of the two models is established. The statistical information of the residual absolute error value is shown in Table 1, which compares the externally coincident precision of the inverse distance weighting (IDW) and Kriging methods under the same resolution conditions.

The internal error is the precision obtained through the compensating computation under optimal estimation is also called the mean square error $\hat{\sigma}$ of the unit weight:

$$\hat{\sigma} = \sqrt{V^T PV / (n_s - t_s)} \tag{8}$$

Where V is the residual error of the evaporation capacity in the observation station involved in the adjustment calculation, n_s is the number of observed values and is set as 23, and t_s is the observed quantity and is set as 10. The externally coincident precision is obtained by calculating the data in the observation station of the externally coincident inspection. The calculation formula is as follows:

$$\hat{\sigma}_{EAA} = \sqrt{\frac{\sum_{k=1}^{3}(ET_{ass} - ET_{real})}{3}} \tag{9}$$

Where $\hat{\sigma}_{EAA}$ is the externally coincident precision; ET_{ass} is the estimated model value of the evaporation capacity in the observation station; and ET_{real} is the known observed value in the observation station.

Table 1

Statistical table of the absolute values of the residual error and precision indexes (unit: mm)

Spherical Function	Time	$v \le 1$	$1 < v \le 1.5$	$1.5 < v \le 2$	$v > 2$	$\hat{\sigma}$	$\hat{\sigma}_{EAA}$	OM	$\hat{\sigma}_{EAA}$
Temperature Not Considered (SHTNC)	1st day	82.6%	13.0%	4.4%	0.0	0.92	1.45	IDW	1.82
	2nd day	78.3%	21.7%	0%	0.0	0.99	0.90		1.79
	3rd day	87.0%	4.4%	4.4%	4.2%	1.01	0.48		1.81
	4th day	87.0%	13.0%	0%	0.0	0.83	0.53		1.73
	5th day	82.6%	8.7%	8.7%	0.0	0.97	0.94		1.77
Temperature Considered (SHTC)	1st day	95.6%	0%	4.4%	0.0	0.94	1.43	Kriging	1.85
	2nd day	73.9%	26.1%	0%	0.0	1.03	1.07		1.72
	3rd day	91.3%	0%	4.4%	4.3%	1.04	0.77		1.79
	4th day	91.3%	8.7%	0%	0.0	0.88	0.49		1.63
	5th day	82.6%	8.7%	8.7%	0.0	1.04	0.96		1.75

Note: v: the absolute value of the residual error; OM: other method; Kriging: the Kriging model for spatial interpolation

The v represents the absolute value of the residual error after the compensating computation of the model. Table 1 shows the statistics of the percentage of the absolute values of the residual error and the number of those involved in the calculation of the model. Based on Table 1, most of the absolute values of the residual error are superior to 1 mm; those over 90% are less than 1.5 mm; and those consisting of only several data points are greater than 1.5 mm. Generally speaking, both the two models can satisfy the requirements of the spatial interpolation of the evaporation capacity. Regardless of the adjustment and residual error of the model, or the internal and external errors, the numerical values are quite close to one another. The data from columns 8 and 10 in Table 1 are also compared. The external coincident precisions of the two models adopted in this paper are superior to the corresponding values of the IDW and Kriging methods.

Careful analysis shows that an inconsistency exists between the distribution laws of the residual error and the precision of the two models. As shown in Table 1, among the continuous five-day interpolation results, with the exclusion of the two-day results, the results from the other four days do not conform with the law that a good residual error distribution corresponds to good model precision. The residual errors with absolute values of less than 1 mm correspond to the spatial interpolation model that considers the temperature and appear more frequently. The model precision indexes are low, and the highest proportion of the residual errors with absolute values of less than 1 mm of the model that considers the temperature is 95.6%. By contrast, the corresponding value of the model that does not consider temperature is 82.6%. Thus, the difference between the values of the two is 13.0%. For the internal error, the former is 0.94, and the latter is 0.92. For the external error, the former is 1.43, and the latter is 1.45. What is worth mentioning is that the residual error distribution corresponds to two interpolation models that are consistent, while the precision index of the model that considers temperature is slightly lower.

Model precision and reliability are two significant indexes for evaluating the interpolation model. Aside from being influenced by their own functional precision, the resulting interpolation precision is also influenced by the precision of the adopted parameters. Generally speaking, the more parameters the model involves, the lower the interpolation results precision are. However, adopting reasonable parameters can enhance model reliability. Temperature parameters are introduced to the spatial interpolation model that considers temperature. Although this slightly lowers the model precision, it optimizes the distribution laws of the residual error, thereby improving model reliability. In terms of the interpolation results of the daily evaporation capacity, the influence of temperature cannot be highlighted because of the small daily evaporation capacity.

Analysis of the precision of the monthly evaporation data and selection of temperature data

The spherical model is used to conduct the spatial interpolation of the daily evaporation capacity from May to August, 2013. The monthly evaporation capacity is then calculated. When the expanded model is used to conduct spatial interpolation, three kinds of temperature data are selected: the daily average temperature, daily maximum temperature, and mininum temperature. By contrast, when the temperature is not considered in the calculation, four kinds of interpolation results can be obtained.

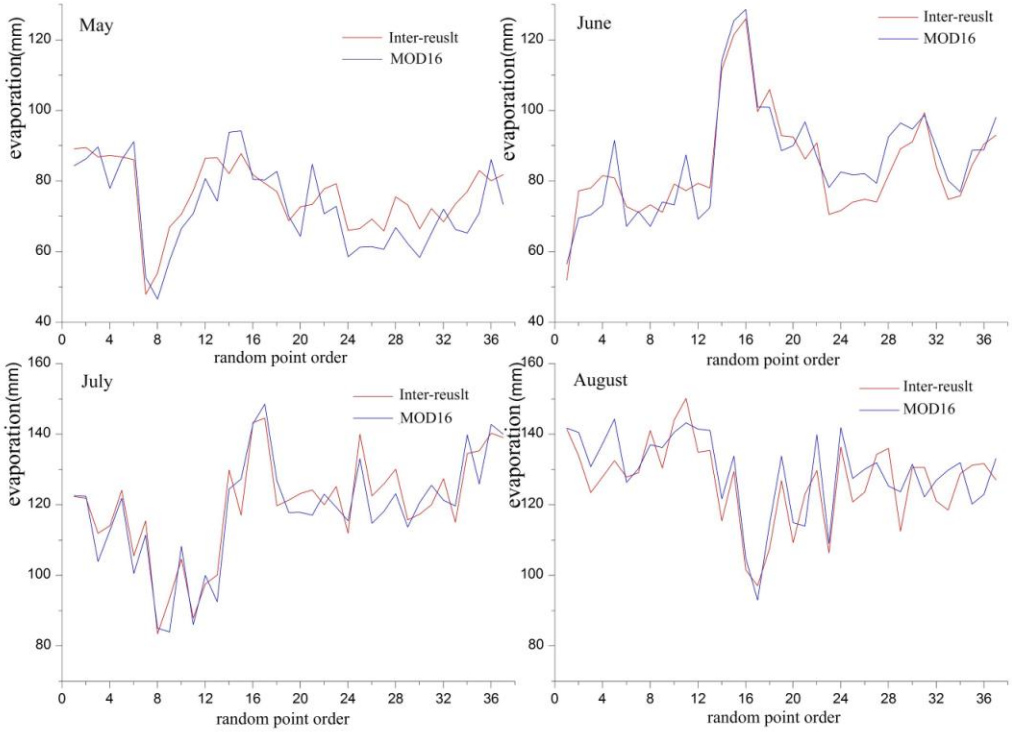

Fig.3 - Comparative diagram of the average temperature interpolation results and MOD16

For 50 randomly generated inspection points, four kinds of interpolation data corresponding to the inspection points are extracted. With the MOD16 data corresponding to the inspection points as the truth value of the evaporation capacity, 37 inspection points data are reserved after the abnormal points on the water surface and urban and town areas are excluded; the variances are calculated and listed in Table 2. A correspondence diagram between the monthly evaporation capacity and MOD16 data, which are obtained by adopting the daily average temperature interpolation, is shown in Fig.3. A comparative diagram between the expanded model and purely spherical function model under the four situations is shown in Fig. 4.

As shown in Fig. 3, the comparison of the monthly evaporation capacities is resolved by expanding the model, which adopts the daily average temperature and MOD16 data. The red line represents the interpolation results, and the blue line represents the MOD16 data. The variation tendencies of the two are consistent, and the interpolation results only jitter up and down the MOD16 data. The maximum error is less than twice the variance. Fig. 4 compares the monthly evaporation capacities of the spherical function models under the four situations. The graph entities for May and July are consistent, but some inspection points exhibit large deviation in June. A large fluctuation with opposite change tendencies occurs in August *(Bezborodov et al. 2010, M.P. Gonzalez et al. 2009)*. Combining the variance data of the evaporation capacities at the inspection points in Table 2, the interpolation data variance in the expanded model, which

uses the daily average temperature, remains stable and small. By contrast, the variances in the interpolation data in other forms are not stable enough. Thus, adopting the daily average temperature as the parameter of the interpolation model can result in relatively ideal interpolation results.

Table 2

Statistical table of the variance in the monthly evaporation data (unit: mm)

Month	DMaxT	DAvgT	DMinT	TE	EMaxError	MOD16
5	6.10	5.98	6.37	6.91	-12.30	93.8
6	4.94	5.05	5.25	7.72	12.25	72.5
7	5.01	5.18	5.47	5.98	-11.72	127.3
8	6.64	5.74	7.51	9.16	14.44	115.0

Note: D: daily; A: average; T: temperature ; TE: temperature excluded; EMaxError :evaporation max error

Given the major hopping position in Fig.4, it is necessary to analyze the characteristics of the temperature data at the test point to study whether the model is practicable for the temperature data. The variance of the model, which takes the average temperature in Table 2 as parameter, is considered to be the threshold value. The inspection point with an error smaller than the threshold value follows a consistent trend, and the inspection point with an error larger than the threshold value is deviation positions. And then the calculation of the statistics of the consistent and deviant positions of the trend corresponding to each month is needed.

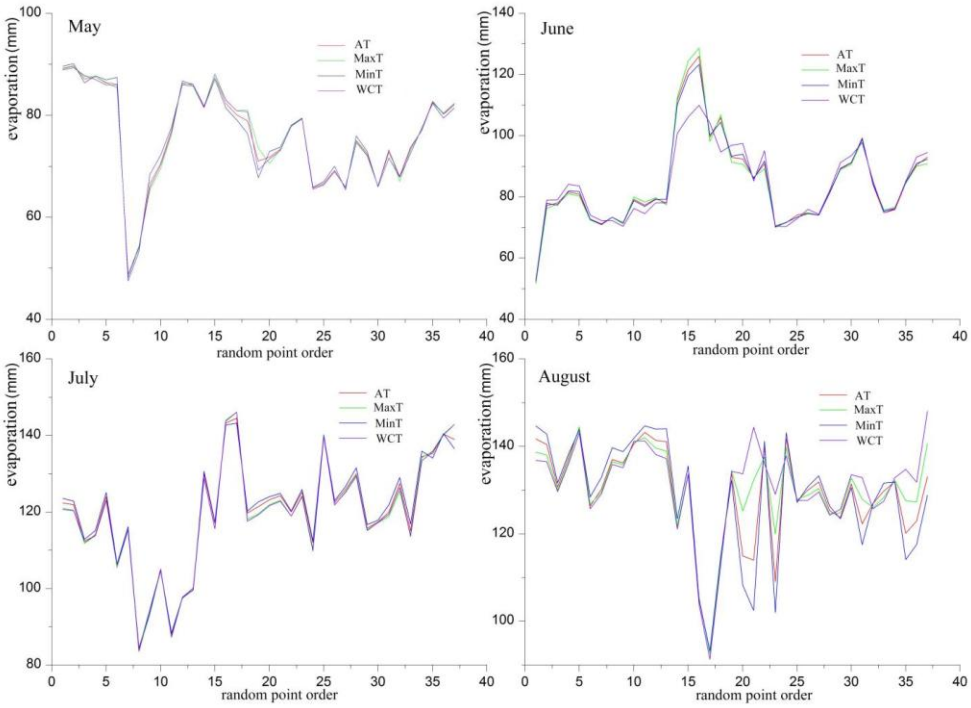

Fig.4 - Comparative diagram of the interpolation results under the four situations

The average maximum temperature, average temperature, average minimum temperature, difference between the average maximum and average minimum temperatures, difference between the average maximum and average temperatures, maximum temperature difference at consistency, and minimum temperature difference at deviation are listed in Table 3.

Table 3

Statistical table of the temperature data characteristics at the inspection points (unit: °C)

M	MAMaxT	AMT	MAMinT	MaxTD	MaxATD	MaxTDC	MinTDD
5	26.71	21.59	17.21	9.50	5.12	4.98	6.47
6	28.45	24.27	20.98	7.47	4.18	3.12	8.58
7	33.99	32.73	30.12	3.87	1.26	4.10	6.23
8	34.29	31.65	25.41	8.88	2.64	3.69	8.98

Note: M: month; A: average; T: temperature; D: difference; DC: difference at consistency; DD: difference at deviation

The data volume matrix in Table 3 is established, and its correlation coefficient matrix is solved. The correlation between columns 7 and 8 in Table 3 with the proceeding columns is observed, and the maximum correlation coefficient is 0.42. Hence, the model interpolation effect does not have any significant linear correlation with the overall variation range of the temperature data or with the temperature. The correlation coefficient between columns 7 and 8 is -0.76, which is a significantly negative correlation. Hence, the data in columns 7 and 8 in Table 3 are combined and taken as the indexes of the model's resistance capability to temperature variations; that is, the interpolation effect is good when the temperature variation is within 3.12 °C, but is poor when the temperature variation is above 6.23°C.

The monthly evaporation interpolation is calculated by transforming the multiple temperature parameters. Through the comparative analysis of the interpolation results and the continuous space–time distribution features of the MOD16 data, the adoption of the daily average temperature can obtain the optimal solution of the model. The variance in the optimal value is taken as the threshold value to classify the interpolation results. The maximum temperature difference at consistency (TDC) and minimum temperature difference at deviation (TDD) can also be obtained. These two are correlated with the interpolation results and can serve as the indexes to evaluate the temperature difference resistance capacity and the applicability of the model.

Accumulation effect of the daily evaporation capacity with consideration of the temperature

The expanded spherical function model, which considers the temperature, produces the accumulation effect of the daily evaporation capacity *(Jiménez-Bello et al. 2011).* The comparation and analysis of the MOD16 data in August with the accumulation effect had been made. As shown in Fig.5, A represents the accumulated monthly value of the spatial interpolation of the daily evaporation without consideration of the temperature, B represents the value with consideration of the temperature, and C represents the MOD16 data.

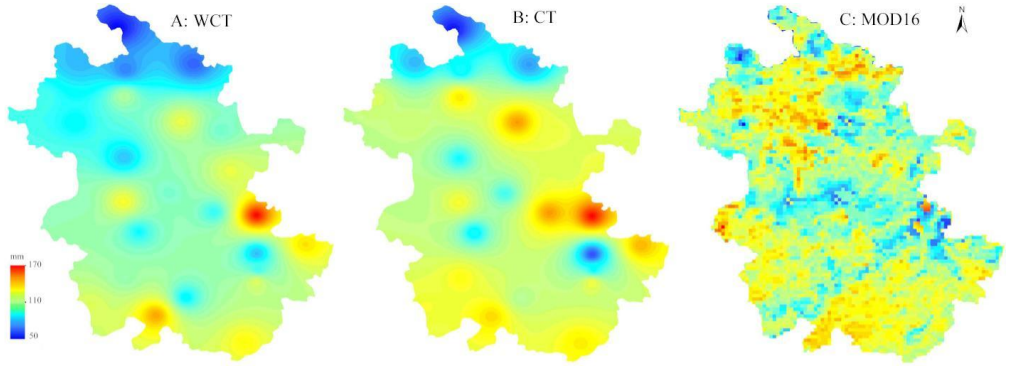

Fig.5 - Monthly cumulative comparison of the spatial interpolation of the evaporation capacity

The overall evaporation data in Fig. 5A are low. Meanwhile, the evaporation distribution in Fig. 5B more closely approaches the data in Fig. 5C than those in Fig. 5A, the evaporation data to the east and west of Anhui Province are higher than those in the corresponding areas in Fig. 5A, which embody the accumulation effect of the spherical function model that considers the temperature. Based on the statistical data of the monthly evaporation capacity during the 4-month spatial expansion in 37 inspection points examined in this study, the temperature accumulation effect may indicate that the sum of the monthly evaporation capacities in the inspection points obtained by the model resolution corresponds to each temperature parameter minus those obtained by the model resolution that does not consider temperature. The difference values are listed in Table 4; column 1 represents the month, columns 2 to 4 represent the difference values of the evaporation capacity, column 5 represents the sum of the evaporation capacities of the inspection points of the model that does not consider temperature, and column 6 represents the MOD16 data.

Table 4

Statistical table of the difference values of the monthly evaporation capacity and relevant data (unit: mm)

M	maxT	AvgT	minT	TE	MOD16
5	5.48	4.32	0.09	2338.568	2346.4
6	22.60	19.48	19.30	2550.447	2591.9
7	35.25	18.49	16.27	4292.903	4263.4
8	9.23	49.67	77.67	3976.740	3998.2

Note: M: month; Avg: average; T: temperature; E: excluded

Based on Table 4, the sum of the monthly evaporation capacities in all the months under all the temperature parameters are greater than the sum of the monthly evaporation capacities resolved by the model that does not consider temperature.

This indicates that the model that considers temperature has a temperature accumulation effect. The difference value matrix of the evaporation capacities from columns 2 to 4 in Table 4 and the temperature data matrix from columns 2 to 4 in Table 3 are established.

The correlation coefficient between the two matrices is 0.251, which indicates that the linear correlation between the temperature accumulation effect and temperature is not obvious.

The correlation coefficient between columns 5 and 6 in Table 4 is 0.997, which indicates that the resolution of the function model has a significant correlation with the MOD16 data.

The temperature accumulation effect exists in the interpolation of monthly evaporation data. However, it is restricted by the spatial density of temperature, observed evaporation value, and data precision. Moreover, given the complicated relationship between temperature and evaporation capacity, this study does only little to reveal the temperature accumulation phenomenon, which should be the focus in future studies.

CONCLUSIONS

To satisfy the requirements of the agricultural environment study for continuous space–time distribution, the calculation of the evaporation spatial interpolation should not be limited to traditional methods, and relevant multi-source information must necessarily be integrated.

This study proposes a new method for the spatial interpolation of the evaporation capacity. It then uses actual measured data in Anhui Province and national temperature field distribution to verify the proposed method and at the same time analyses the influence of the temperature field on the interpolation results.

The following conclusions can be drawn from the study:

- Error analysis indicates that this method has high precision and is superior to the pure IDW and KRIGING methods. The introduction of temperature parameters results in inconsistencies between the distribution law of the residual error of the interpolation results and the internal and external errors. This occurs because, after the temperature parameters are introduced to the spatial interpolation model, the errors of the temperature parameters are propagated and affect the model precision. However, the interpolation results lead to a more optimal distribution, thereby enhancing the reliability of the model;
- Based on the analysis, the TDC and TDD are correlated with the interpolation results. They can serve as indexes for the model temperature difference resistance ability and evaluation of the model applicability. Taking the MOD16 monthly evaporation capacity with continuous space–time distribution features as the control, this paper analyses the monthly evaporation interpolation results under multiple temperature values and adopts the daily average temperature to conduct model resolution and obtain the optimal solution;
- In the calculation of the spatial expansion of the monthly evaporation capacity, the model that considers temperature exhibits the temperature accumulation effect phenomenon, and it has a more complicated relationship with the daily evaporation data.

This study satisfies the required evaporation data for agricultural environment and provides a reference and basis for the calculation of field evaporation data and analysis of the relationship between temperature and field evaporation. This promotes farmland water management and utilization, as well as relevant progress in agricultural production. However, evaporation, which is a complicated natural phenomenon, has a complex relationship with factors, such as altitude, wind speed, and temperature. Further analysis must be conducted on the influence of all these factors on the method proposed in this study.

ACKNOWLEDGEMENT

The work was supported by the National Science and Technology Pillar Program during the 12th “Five-Year Plan” Period (Project No.: 2012BAD08B03-4)

REFERENCES

[1] Bezborodov G. A., Shadmanov D. K., Mirhashimov R. T., et al., (2010), Mulching and water quality effects on soil salinity and sodicity dynamics and cotton productivity in Central Asia, *Agriculture, Ecosystems & Environment,* Elsevier B.V./ America, Vol.138, Issue.1-2, ISSN 0167-8809, pp.95-102;

[2] Cha Weiwei, Liu Yu., Liu Yulong. etc., (2013), Regional evaporation and transpiration simulation and verification and remote sensing based on SWAT model, *Journal of China Institute Water Resource and Hydropower Research,* Vol.11, Issue 3, pp.167-175, ISSN 1672-3031, China Institute of Water Resources and Hydropower Research, Beijing;

[3] Gonzalez-Dugo M. P., Neale C. M. U., et al., (2009), A Comparison of Operational Remote Sensing-based Model for Estimating Crop Evapotranspiration. *Agricultural and Forest Meteorology*, Elsevier B.V., Vol.149, Issue 11, pp.1843-1853, ISSN 0168-1923;

[4] Hassan M., (2013), Evaporation estimation for Lake Nasser based on remote sensing technology, *Ain Shams Engineering Journal*, Vol.4, Issue 4 , pp.593-604, Ain Shams University, Cairo;

[5] Jin Y. L., Huang J. S., Wang X. G, (2014), Identification of waterlogged field based on multi-source data, *Engineering Journal of Wuhan University*, Vol.47, Issue 3, pp.289-293, ISSN 1671-8844, Wuhan University, Wuhan / China,;

[6] Jiménez-Bello M. Á., Alzamora F. M., Castel J. R., et al.,(2015), Validation of a methodology for grouping intakes of pressurized irrigation networks into sectors to minimize energy consumption. *Agricultural Water Management*, Elsevier B.V./ America, Vol.102 , Issue 1, pp.46-53; ISSN 0378-3774,

[7] Lagos L. O., Martin D. L., Verma S.B., et al., (2013), Surface energy balance model of transpiration from variable canopy cover and evaporation from residue-covered or bare soil systems: model evaluation, *Irrigation Science*, Springer- Verlag, Berlin/Germany, Vol.31, Issue 2 , pp.135-150, ISSN 0342-7188;

[8] Li Xianghu, Zhang Qi, Ye Xuchun, (2013), The effects of spatial distribution of Different soil physical properties on hydrological processes modelling, *Journal of Soil and Water Conservation*, Vol.33, Issue 05, pp.190-195, ISSN 0022-4561, Soil Water Conservation Society, Ankeny;

[9] Paul D. C., William P.K., Martha C. A., et al., (2012), Two-source energy balance model estimates of evapotranspiration using component and composite surface temperatures, *Advances in Water Resources*, Vol.50, Issue 3, pp.134-151, ISSN 0309-1708, Loughborough University, Leicestershire;

[10] Qian Long, Wang Xiugui, Luo Wenbing, (2015), Yield reduction analysis and determination of drainage index in cotton under waterlogging followed by submergence, *Transactions of the Chinese Society of Agricultural Engineering*, vol.31, Issue 13, pp.89-97, ISSN 1002-6819, Chinese Society of Agricultural Engineering, Beijing;

[11] Raghuveer K. V., Eric F. W., Craig R. F., et al., (2011), Global estimates of evapotranspiration for climate studies using multi-sensor remote sensing data: Evaluation of three process-based approaches, *Remote Sensing of Environment*, Elsevier B.V./America, vol.115, Issue 3, pp.801-823, ISSN 0034-4257;

[12] Seitz F., Schmidt M., Shum C. K., (2008), Signals of extreme weather conditions in Central Europe in GRACE 4-D hydrological mass variations, *Earth and Planetary Science Letters*, Elsevier B.V./America, vol. 268, Issue1-2, pp.165 -170, ISSN 0012-821X;

[13] Su T., Feng G. L., (2015), Spatial-temporal variation characteristics of global evaporation revealed by eight reanalyses, *Science China Earth Sciences*, Science China Press , Beijing, vol.58, Issue 2, pp.255-269, ISSN 1674-7313;

[14] Tian F., Qiu G. Y., Yang Y. H., et al., (2013), Estimation of evapotranspiration and its partition based on an extended three-temperature model and MODIS products, *Journal of Hydrology*, Elsevier B.V./ America , Vol. 498, Issue1-4, pp.210- 220, ISSN 0022-1649;

[15] Yang D.J., (2011), *Soil water dynamics model and its application on SPAC system modelling*, vol.1, pp.78-110, ISBN 9787308092746,, Zhejiang University Press, Hangzhou.